Cascades of π Circuits Modeled by Independent Matrix Equations for Each Infinitesimal Unit

A. J. Prado[1], **L. S. Lessa**[2], **R. C. Monzani**[3], **L. F. Bovolato**[2], **J. Pissolato Filho**[3], **E. Assunção**[2], **and M. C. M. Teixeira**[2]

[1]Telecommunication Engineering Department, Campus of S. J. Boa Vista
Univ. Estadual Paulista — UNESP, Brazil
[2]Electrical Engineering Department, Campus of Ilha Solteira
Universidade Estadual Paulista — UNESP, Brazil
[3]Electrical Engineering Department
The State University of Campinas — UNICAMP, Brazil

Abstract— A modified numeric procedure is applied to analyse the application of π circuits for representing distributed parameters. Numeric oscillations, which are associated usually with digital simulations associated with π circuits, are decreased. It is shown that these numeric oscillations, or Gibb's oscillations, are not related only to the mentioned associations. They are created by the application of the specific numeric integration methods for solving linear systems that describe the associations of π circuits. If the state equations are determined for each π circuit, then the proposed changes of the numeric routine for solving systems with π circuits lead to results with little influence on the numerical oscillations. This is confirmed using comparisons with results obtained from the Laplace transform and ATP software.

1. INTRODUCTION

For simulating transient phenomena and wave propagation in electrical power systems, digital programs and numerical tools are useful. This is because tests in actual systems can be impossible, for example, in actual transmission lines [1], or very difficult, because the results have very high frequencies, for example, during signal propagation in integrated circuits. For infinitesimal representation of systems with distributed parameters, lumped elements can be applied, using structures of π circuits [2–7]. With a great number of these infinitesimal units, it can provide good representations of these systems. There can be problems caused by numeric integration methods [8–10]: numerical oscillations. These numerical oscillations, called Gibb's oscillations, are produced by numeric integration methods related to associations of π circuits [1–10]. The cascade of π circuits is included in numeric routines as a space state matrix generated from the π circuit's state variables [2–7]. The order of the mentioned matrix depends on the number of π circuits applied. Applying n π circuits, it is necessary to have a $2n$-order matrix in the numeric routine. The increase of the order of the mentioned matrix is not related directly to a corresponding reduction of Gibb's oscillations [2–7, 10, 18, 19]. Searching for a simple representation of the cascade of π circuits, each unit is modelled individually [18, 19]. The influence of adjacent π circuit units are included by the differential relations among the state variables. Thus, the Gibb's oscillations are decreased significantly. The proposed numeric routine is more accurate than the numeric routine based on the application of only one matrix for representing the dynamics of π circuits [20, 21].

2. ANALYSES OF A CASCADE OF π CIRCUITS

A cascade of π circuits can be used for mono-phase representations of transmission lines. One unit of π circuit can be considered an infinitesimal unit of a line representation. The unit of π circuit is a first order filter [2–7]. For infinitesimal transmission line representations, the length of influence of the each π circuit unit on the voltage and current is introduced by an infinitesimal distance (Δx). The mentioned cascade is described as a linear system solved numerically [2–7, 10, 18, 19]:

$$\dot{x} = Ax + Bu \tag{1}$$

In (1), A is the matrix associated with the electrical system, B is the matrix or vector related to the sources, x is the vector of the state variables, and u is the vector of the inputs. If the cascade of π circuits is opened at the receiving end terminal, the structure of matrix A is as shown in (2) for a voltage source connected to the sending end terminal. The matrix A is calculated by [2–7]:

$$A = \begin{bmatrix} 1/L & -R/L & 0 & \dots & \dots & 0 & \\ 0 & 1/C & -G/C & -1/C & 0 & \dots & \vdots \\ 0 & 0 & 1/L & -R/L & -1/L & 0 & \vdots \\ \vdots & \ddots & \ddots & \ddots & \ddots & \ddots & \vdots \\ \vdots & \ddots & \ddots & \ddots & \ddots & \ddots & 0 \\ \vdots & \ddots & \ddots & 0 & 1/L & -R/L & -1/L \\ 0 & \dots & \dots & \dots & 0 & 2/C & -G/C \end{bmatrix} \tag{2}$$

The elements in (2) are determined from [2, 3]:

$$R = \frac{R' \cdot d}{n} \quad L = \frac{L' \cdot d}{n} \quad C = \frac{C' \cdot d}{n} \quad G = \frac{G' \cdot d}{n} \tag{3}$$

Calculating the eigenvalues of matrix A, it is obtained that:

$$\begin{aligned} &\lambda = \begin{bmatrix} -\frac{G}{C} & -\frac{R}{L} + \frac{2}{\lambda_1 LC} & -\frac{G}{C} + \frac{1}{\lambda_2 LC} & \dots & A_{kk} + \frac{1}{\lambda_{k-1} LC} & \dots & -\frac{R}{L} + \frac{1}{\lambda_{n-1} LC} & -\frac{G}{C} + \frac{2}{\lambda_n LC} \end{bmatrix}^T \\ &k = 4, \dots, 2n-1 \quad \rightarrow \quad \text{If } k \text{ is even, } A_{kk} = -\frac{R}{L}. \quad \text{If } k \text{ is odd, } A_{kk} = -\frac{G}{C}. \end{aligned} \tag{4}$$

Because the R, L, G, and C values are positive and real, the λ_1 value is real and negative. Based on the λ_1 value, each λ_k value depends on the previous eigenvalue and it is also real and negative. From (4) and (2), all eigenvalues of matrix A are real and negative. So, the linear system in (1) is a stable system. If Heun's method is used to simulate the wave propagation of a voltage step through the cascade of π circuits, the obtained results are as shown in Figs. 2–7 and based on [2]:

$$\begin{aligned} x(k+1) &= \left[I - \frac{\Delta t}{2} A\right]^{-1} \left\{ \left[I + \frac{\Delta t}{2} A\right] x(k) + \frac{\Delta t}{2} \left[u(k+1) + u(k)\right] \right\} \\ x &= \begin{bmatrix} i_1 & v_1 & i_2 & v_2 & \dots & i_n & v_n \end{bmatrix}^T \end{aligned} \tag{5}$$

In (5), Δt is the time step of the trapezoidal rule, $x(k)$ is the known values of the state variables, and $x(k+1)$ represents the new values of the state variables that are calculated from $x(k)$. The u vector has non-null elements for those points where the sources are connected. For the obtained results, the values of the line parameters are [2, 3]: $R' = 0.05\,\Omega/\text{km}$, $L' = 1\,\text{mH/km}$, $G' = 0.556\,\mu\text{S/km}$, and $C' = 11.11\,\text{nF/km}$. The other values are: $d = 5\,\text{km}$, $t_{\text{MAX}} = 60\,\text{ms}$ and $\Delta t = 50\,\text{ns}$.

Analyzing the results shown in this section (Figs. 1–2), it is observed that the changes in the number of π circuits and the time steps cannot modify the overvoltage value of the simulations performed. There are no modifications in the voltage peak values reached after voltage damping. With an increase of the number of π circuits or a decrease in the time step, the voltage peak values are about *2.03 pu*. The proceedings checked in this section can only modify the frequency of the Gibb's oscillations.

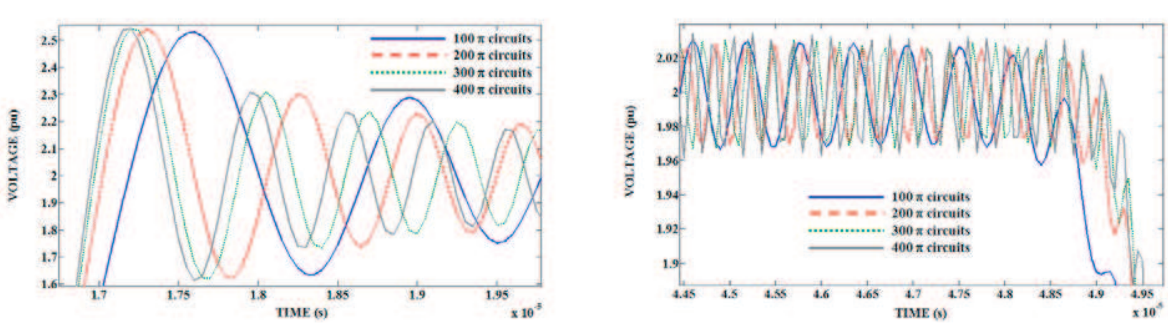

Figure 1: Voltage step propagation for different quantities of circuits using the state equation for the cascade of π circuits.

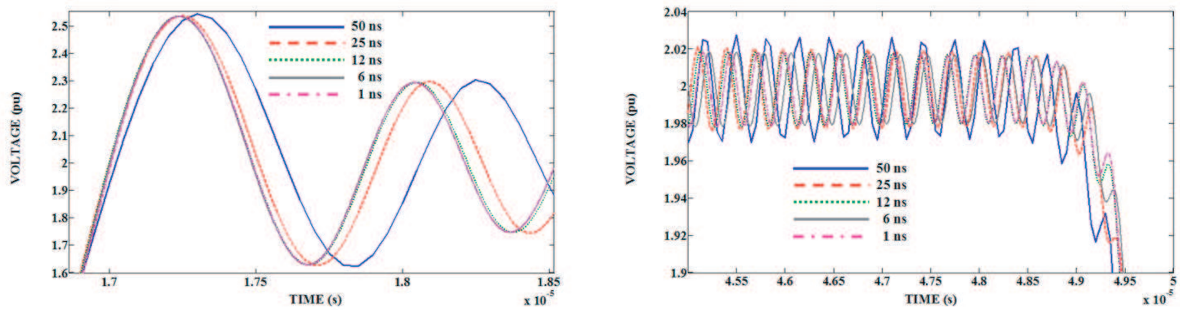

Figure 2: Voltage step propagation for different time steps using the state equation for the entire cascade of π circuits.

3. ROUTINE FOR ANALYSES OF EACH π CIRCUIT

The characteristic π circuits, shown in Fig. 3, are applied for all π circuits of the cascade. Only the first and the last π circuits are different of the other π circuits. From the second to the penultimate π circuits, the related state equation is given in (6) and its elements are in given in (7).

$$\dot{x_j} = A_\pi \cdot x_j + D i_{j+1} + E v_{j-1}, \quad j = 2, \ldots, n-1 \tag{6}$$

$$A_\pi = \begin{bmatrix} -R/L & -1/L \\ 1/C & -G/C \end{bmatrix} \quad E = \begin{bmatrix} 1/L \\ 0 \end{bmatrix} \quad D = \begin{bmatrix} 0 \\ -1/C \end{bmatrix} \quad x_j = \begin{bmatrix} i_j \\ v_j \end{bmatrix} \tag{7}$$

Applying the trapezoidal rule, it is obtained that:

$$x_j\,(k+1) = x_j(k) + \frac{\Delta t}{2}\left[\dot{x_j}\,(k+1) + \dot{x_j}(k)\right] \tag{8}$$

Both the vectors for x_j for different times are given in (9); there are two unknown values. One of these unknown values is the term $v_{j-1}(k)$ that has just changed into $v_{j-1}(k+1)$ for the previous π circuit. The term $i_{j+1}(k+1)$ cannot be determined without the actualisation of $v_j(k)$ and $i_j(k)$.

$$\dot{x_j}\,(k+1) = A_\pi \cdot x_j\,(k+1) + D i_{j+1}\,(k+1) + E v_{j-1}\,(k+1) \qquad \dot{x_j}(k) = A_\pi \cdot x_j(k) + D i_{j+1}(k) + E v_{j-1}(k) \tag{9}$$

For the $v_{j-1}(k)$ and $i_{j+1}(k+1)$ unknown values, it is used:

$$\frac{di_j}{dt} = \frac{1}{L} v_{j-1} - \frac{R}{L} i_j - \frac{1}{L} v_j \rightarrow v_{j-1} = L\frac{di_j}{dt} + R i_j + v_j \tag{10}$$

For calculating the term $i_{j+1}(k+1)$, it is used:

$$\frac{\Delta i_j}{\Delta t} \cong \frac{di_j}{dt} = \frac{1}{L} v_{j-1} - \frac{R}{L} i_j - \frac{1}{L} v_j \tag{11}$$

Based on (12), the term $i_{j+1}(k+1)$ is:

$$\begin{aligned} i_{j+1}\,(k+1) &= i_{j+1}(k) + \Delta i_{j+1}(k) \cong i_{j+1}(k) + \frac{\Delta t}{L} v_{j-1}(k) - \frac{R\Delta t}{L} i_{j+1}(k) - \frac{\Delta t}{L} v_{j+1}(k) \\ &= \frac{\Delta t}{L} v_{j-1}(k) + \left(1 - \frac{R\Delta t}{L}\right) i_{j+1}(k) - \frac{\Delta t}{L} v_{j+1}(k) \end{aligned} \tag{12}$$

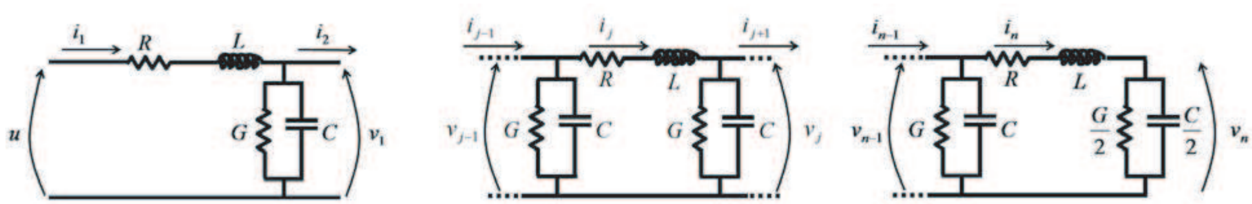

Figure 3: Structure of characteristic π circuits.

The relations in (11) and (12) are true when Δt is very small. With very small Δt, the next relation is:

$$v_{j-1}(k) \cong L\frac{i_j(k+1)-i_j(k)}{\Delta t}+Ri_j(k)+v_j(k) \tag{13}$$

Introducing (14) and (15) in (11), it is obtained that:

$$x_j(k+1)=M_5\left\{M_6x_j(k)+M_7x_{j-1}(k+1)+M_3x_{j+1}(k)+M_4\left[u_{CH}(k+1)+u_{CH}(k)\right]\right\} \tag{14}$$

In (14), the matrices are:

$$M_5=\left[I-\frac{\Delta t}{2}A_{CH3}\right]^{-1}\quad M_6=\left[I+\frac{\Delta t}{2}A_{CH2}\right]\quad M_7=\frac{\Delta t}{2}E\quad M_3=\frac{\Delta t}{2}D_{CH1}\quad M_4=\frac{\Delta t}{2}B_{CH1} \tag{15}$$

The modified A matrices are:

$$A_{CH2}=\begin{bmatrix}-1/\Delta t & 0\\ 1/C & -1/C\cdot(G+\Delta t/L)\end{bmatrix}\quad A_{CH3}=\begin{bmatrix}-R/L+1/\Delta t & -1/L\\ 1/C & -G/C\end{bmatrix} \tag{16}$$

The other matrices and vectors are:

$$B_{CH1}=\begin{bmatrix}1/L & 0\\ 0 & 1/C\end{bmatrix}\quad u_{CH}=\begin{bmatrix}u_j\\ i_{Fj}\end{bmatrix}\quad D_{CH1}=-1/C\cdot\begin{bmatrix}0 & 0\\ 2-R\Delta t/ & -\Delta t/L\end{bmatrix} \tag{17}$$

For the first and the last units, it is obtained that:

$$\dot{x_1}=A_\pi\cdot x_1+B_{1\pi}u+Di_2\quad \dot{x_n}=A_{n\pi}\cdot x_n+Ev_{n-1} \tag{18}$$

Applying Heun's method, it is obtained that:

$$\begin{aligned}x_1(k+1)&=M_1\left\{M_2x_1(k)+M_3x_2(k)+M_4\left[u_{CH}(k+1)+u_{CH}(k)\right]\right\}\\ x_n(k+1)&=M_8\left\{M_9x_n(k)+M_7x_{n-1}(k+1)+M_4\left[u_{CH}(k+1)+u_{CH}(k)\right]\right\}\end{aligned} \tag{19}$$

In (19), the unknown elements are:

$$M_1=\left[I-\frac{\Delta t}{2}A_\pi\right]^{-1}\quad M_2=\left[I+\frac{\Delta t}{2}A_{CH1}\right]\quad M_8=\left[I-\frac{\Delta t}{2}A_{CH5}\right]^{-1}\quad M_9=\left[I+\frac{\Delta t}{2}A_{CH4}\right] \tag{20}$$

The new A matrices are given in (21). In the case of the A_π and $A_{n\pi}$ matrices, the eigenvalues shown in the vector forms are in (22). The determined eigenvalues are always real and negative values. Each linear system related to the corresponding π circuit unit is a stable system.

$$\begin{aligned}A_{CH1}&=\begin{bmatrix}-R/L & -1/L\\ 1/C & -1/C\cdot(G+\Delta t/L)\end{bmatrix}\quad A_{CH4}=\begin{bmatrix}-1/\Delta t & 0\\ 2/C & -G/C\end{bmatrix}\\ A_{CH5}&=\begin{bmatrix}-R/L+1/\Delta t & -1/L\\ 1/C & -G/C\end{bmatrix}\end{aligned} \tag{21}$$

$$\lambda_{A\pi}=\begin{bmatrix}-\frac{R}{L}\\ -\frac{1}{RC}(RG+1)\end{bmatrix}\quad \lambda_{An\pi}=\begin{bmatrix}-\frac{R}{L}\\ -\frac{1}{RC}(RG+2)\end{bmatrix} \tag{22}$$

In Fig. 4, the flowchart for applying numerically the proposal carried out in this section is presented.

In Figs. 5–6, the results obtained with the equations proposed in this section and summarised in the flowchart of Fig. 4 are shown. Compared with Figs. 1–2, it can be seen that the curve for 333π circuits does not have numerical oscillations. It can be observed for an application of 333π circuits that the overvoltage is reduced significantly from about 25% to about 2.5%. The curves for 200 and 300π circuits present lower overvoltage values than the corresponding curves in Figs. 1–2. Similarly, the voltage damping values for the curves of 200 and 300π circuits are faster than the corresponding curves.

For the results obtained in this section, there are limits to the numerical stability related to the number of π circuits and the time step. Considering a time step of 50.0481 ns, the mentioned limit is 333π circuits. Also, using 333π circuits with higher time steps than the considered time step, gives inadequate results. Numerical stability is associated with the relation between the number of π circuits and the time step that leads to the lowest overvoltage and the fastest voltage damping for the results shown in this section. The time step of 50 ns is suggested for teaching power system transients with the use of a personal computer [2].

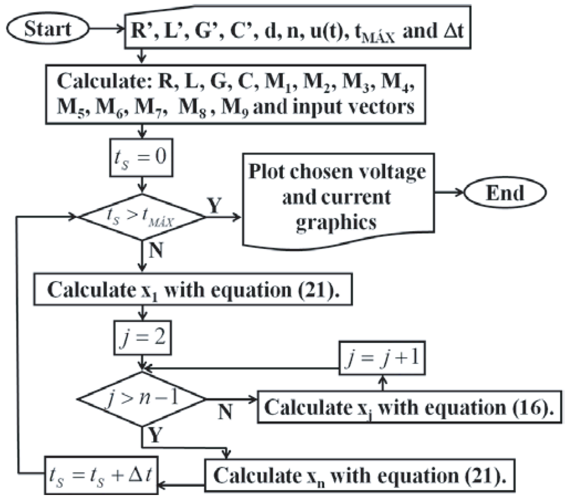

Figure 4: Flowchart of the proposed numeric routine.

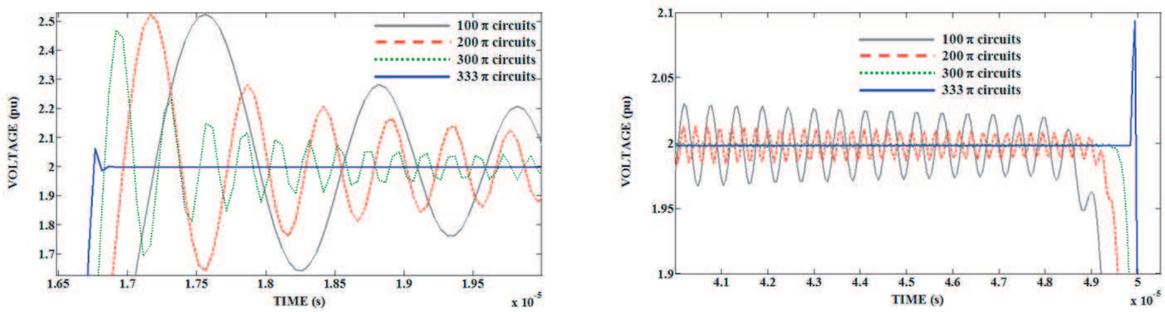

Figure 5: The wave propagation voltage step for different quantities of π circuits using state equations for each π circuit.

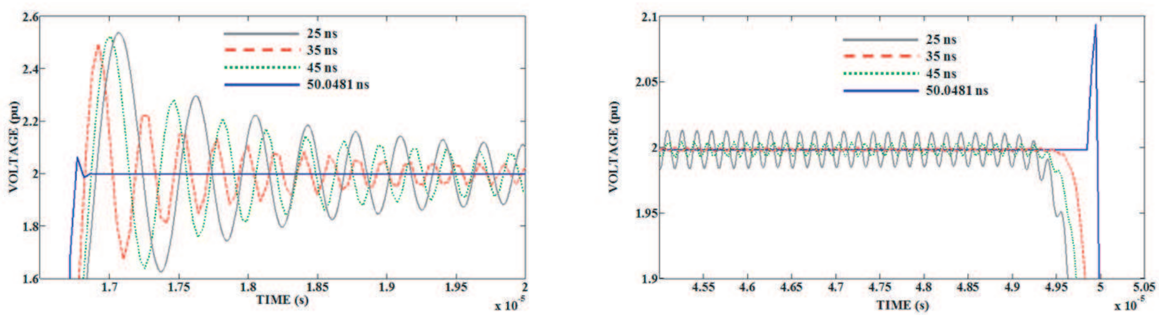

Figure 6: Wave propagation voltage step for different time steps using state equations for each π circuit.

4. CONCLUSION

A modified numeric routine for the application of the trapezoidal integration, or Heun's method for modelling associations of π circuits is presented and analyzed. This numeric routine is applied to simulate the propagation of wave and electromagnetic phenomena through a cascade of π circuits. The proposed changes in the numeric application are based on 2-order matrices for representing each π circuit unit. An important characteristic of the applied 2-order matrices is that these matrices do not have null elements. The results are investigated for a mono-phase representation of a transmission line that is connected to a voltage step input. Analyzing the obtained voltage output, the proposed numeric routine leads to results showing that the numeric oscillations are decreased. Comparing the proposed numeric routine with the unmodified routine used previously for this type of simulation, the reduction in the peaks of the numeric oscillations is about ten times. The previous unmodified numeric routine uses only one $2n$-order matrix to represent the entire cascade with $n\pi$

circuits. This implies that for a specific instant of the simulation, all variables are determined using relations between the $2n$-matrices and the inverse $2n$-order matrices. Therefore, the main change is the method of the application of the numeric integration. Using the same numeric integration method applied to the unmodified numeric routine, the overshot values are only about 3% higher than the voltage output for the proposed numeric routine. This is a decrease of about ten times in these undesirable numeric oscillations. These oscillations are damped in only three time steps.

ACKNOWLEDGMENT

This work was supported by FAPESP (São Paulo Research Foundation) and CNPq (Council for Scientific and Technological Development).

REFERENCES

1. Dommel, H. W., *Electromagnetic Transients Program — Rule Book*, Oregon, 1984.
2. Nelms, R. M., G. B. Sheble, S. R. Newton, and L. L. Grigsby, "Using a personal computer to teach power system transients," *IEEE Trans. on Power Systems*, Vol. 4, No. 3, 1293–1294, Aug. 1989.
3. Nelms, R. M., S. R. Newton, G. B. Sheble, and L. L. Grigsby, "Simulation of transmission line transients using a personal computer," *IEEE Conference Record of the 1988 Eighteenth Power Modulator Symposium*, 229–232, Hilton Head, South Carolina, USA, Jun. 20–22, 1998.
4. Mamis, M. S., "Computation of electromagnetic transients on transmission lines with nonlinear components," *IEE Proc. Generation, Transmission and Distribution*, Vol. 150, No. 2, 200–204, Mar. 2003.
5. Mamis, M. S. and M. Koksal, "Transient analysis of nonuniform lossy transmission lines with frequency dependent parameters," *Electric Power Systems Research*, Vol. 52, No. 3, 223–228, Dec. 1999.
6. Mamis, M. S. and M. Koksal, "Solution of eigenproblems for state-space transient analysis of transmission lines," *Electric Power Systems Research*, Vol. 55, No. 1, 7–14, Jul. 2000.
7. Mamis, M. S. and M. E. Meral, "State-space modeling and analysis of fault arcs," *Electric Power Systems Research*, Vol. 76, No. 1–3, 46–51, Sep. 2005.
8. Macías, J. A. R., A. G. Expósito, and A. B. Soler, "A comparison of techniques for state-space transient analysis of transmission lines," *IEEE Trans. on Power Delivery*, Vol. 20, No. 2, 894–903, Apr. 2005.
9. Macías, J. A. R., A. G. Expósito, and A. B. Soler, "Correction to 'A comparison of techniques for state-space transient analysis of transmission lines,"' *IEEE Trans. on Power Delivery*, Vol. 20, No. 3, 2358, Jul. 2005.
10. Prado, A. J., S. Kurokawa, J. Pissolato Filho, L. F. Bovolato, and E. C. M. Costa, *Phase-mode Transformation Matrix Application for Transmission Line and Electromagnetic Transient Analyses*, Nova Science Publisher, Inc., Hauppauge, NY, 2011.
11. Morched, A., B. Gustavsen, and M. Tartibi, "A universal model for accurate calculation of electromagnetic transients on overhead lines and underground cables," *IEEE Trans. on Power Delivery*, Vol. 14, No. 3, 1032–1038, Jul. 1999.
12. Brandão Faria, J. A., "Overhead three-phase transmission lines — Non-diagonalizable situations," *IEEE Trans. on Power Delivery*, Vol. 3, No. 4, Oct. 1988.
13. Brandão Faria, J. A. and J. Briceño Mendez, "Modal analysis of untransposed bilateral three-phase lines — A perturbation approach," *IEEE Trans. on Power Delivery*, Vol. 12, No. 1, Jan. 1997.
14. Brandão Faria, J. A. and J. Briceño Mendez, "On the modal analysis of asymmetrical three-phase transmission lines using standard transformation matrices," *IEEE Trans. on Power Delivery*, Vol. 12, No. 4, Oct. 1997
15. Wedepohl, L. M., H. V. Nguyen, and G. D. Irwin, "Frequency-dependent transformation matrices for untransposed transmission lines using Newton-Raphson method," *IEEE Trans. on Power Systems*, Vol. 11, No. 3, 1538–1546, Aug. 1996.
16. Nguyen, T. T. and H. Y. Chan, "Evaluation of modal transformation matrices for overhead transmission lines and underground cables by optimization method," *IEEE Trans. on Power Delivery*, Vol. 17, No. 1, Jan. 2002.
17. Marti, J. R., "Accurate modelling of frequency-dependent transmission lines in electromagnetic transients simulations," *IEEE Trans. on PAS*, Vol. 101, 147–155, Jan. 1982.

18. Monzani, R. C., A. J. Prado, S. Kurokawa, L. F. Bovolato, and J. Pissolato Filho, "Using a low complexity numeric routine for solving electromagnetic transient simulations," *Matlab — A Fundamental Tool for Scientific Computing and Engineering Applications*, 463–484, InTech-Open Access Publisher, Rijeka, Croatia, 2012, DOI 10.5772/48507.
19. Lessa, L. S., A. J. Prado, S. Kurokawa, L. F. Bovolato, and J. Pissolato Filho, "The MatLab software application for electrical engineering simulations and power system analyses," *MatLab — A Fundamental Tool for Scientific Computing and Engineering Applications*, 433–462, InTech-Open Access Publisher, Rijeka, Croatia, 2012, DOI 10.5772/48555.
20. Moreno, P. and A. Ramirez, "Implementation of the numerical Laplace transform: A review," *IEEE Trans. on Power Delivery*, Vol. 23, No. 4, Oct. 2008.
21. Prikler, L. and H. K. Hoidalen, *ATPDraw Version 3.5 — Users' Manual*, Trondheim, Norway, Aug. 2002.
22. Dommel, H. W., *EMTP Theory Book*, 2nd Edition, Vancouver, Apr. 1996.
23. Martí, J. R. and J. Lin, "Supression of numerical oscillations in the EMTP," *IEEE Trans. on Power Systems*, Vol. 4, No. 2, May 1989.
24. Lin, J. and J. R. Martí, "Implementation of the CDA procedure in the EMTP," *IEEE Trans. on Power Systems*, Vol. 5, No. 2, May 1990.